

Stretchable slide-ring supramolecular hydrogel for flexible electronic devices

Shuaipeng Wang¹, Yong Chen¹, Yonghui Sun¹, Yuexiu Qin¹, Hui Zhang¹, Xiaoyong Yu¹ & Yu Liu¹  

Slide-ring materials with movable cross-links have received attention due to their excellent mechanical properties. However, due to the poor solubility of polyrotaxane and low synthesis efficiency, their applications are hindered. Here, we use hydroxypropyl-modified α -cyclodextrin (Hy- α -CD) and Acrylamide-PEG₂₀₀₀₀-Acrylamide (ACA-PEG₂₀₀₀₀-ACA) to construct a polypseudorotaxane with good water solubility. Through photo-initiated polymerization of polypseudorotaxane with acrylamide in-situ, the capped polyrotaxane was easily obtained and further cross-linked by 1,4-butanediol diglycidyl ether in sodium hydroxide solution to form a slide-ring supramolecular hydrogel. The hydrogel can be stretched to 25.4 times its original length, which recovers rapidly on unloading, and the addition of Ca²⁺ ions during crosslinking enhances ionic conductivity. The Ca²⁺-doped hydrogels are used to prepare wearable strain sensors for monitoring human motion.

¹College of Chemistry, State Key Laboratory of Elemento-Organic Chemistry, Nankai University, Tianjin 300071, P. R. China. ✉email: yuliu@nankai.edu.cn

Hydrogels are natural or synthetic polymer networks that swell in water and are mechanically, chemically and electrically compatible with biological tissues^{1,2}. The high water content (over 95% by weight ratio) and high diffusivity enable the hydrogel to dissolve and transport ions and many small molecules. Therefore, hydrogels have an irreplaceable position in the fields of cell engineering, drug loading and bioengineering³. For example, soft and elastic hydrogels are widely used in flexible sensors^{4–8}, flexible robots^{9–11} and other fields^{12–14} due to their excellent flexibility^{15–17}, ductility¹⁸, anti-fatigue performance¹⁹, ease of preparation²⁰, stimulus responsiveness²¹, and rich functional expansibility^{22,23}. However, most of traditional hydrogel materials have relatively low mechanical properties, and then these materials are difficult to withstand the high stress, high strain, impact load or cyclic load that may occur in production practice, which greatly restricted their applications. Therefore, how to prepare a hydrogel with high stretchability, fatigue resistance and high water content remains a challenge. Recently, many attempts including dual network, ionic crosslinking, freeze-thaw cycles, stretching, and mechanical training have been tried to improve the mechanical properties of traditional hydrogels^{24,25}. Nevertheless, many hydrogels with the same high water content do not simultaneously exhibit high strength, toughness and fatigue resistance.

Wherein slide-ring gels with movable crosslinks (also called polyrotaxane gels) have attracted much attention as a new type of polymer gel^{26–28}. This type of gel network is topologically cross-linked by the ring structures, such as α -cyclodextrin (α -CD), to form figure-eight cross-linked polymer chains²⁹. The main difference between the traditional chemical cross-linking gel and slide-ring gel is as follow. The polymer obtained by cross-linking with traditional chemical cross-linking agent has a fixed chemical cross-linking point. Under the action of external force, the gel polymer segment is not uniformly stressed, which will destroy the network structure. However, for slide-ring gel, when subjected to the external force, the ring structure, as the crosslinking point, can slide along the polymer chain like a “pulley”. The “pulley” effect makes the internal stress evenly distributed to each chain segment and then to the whole network. This unique “pulley effect” gives the slide-ring hydrogel excellent mechanical properties^{30–32}, such as extremely soft characteristics, relatively low initial modulus and higher ductility.

Although slide-ring materials have excellent mechanical properties, its production and application are greatly limited due to the relatively low solubility of polypseudorotaxane in water as well as the complicated end-capping process of rotaxane. In this work, the polyacrylamide used as capping can form a relatively stable network structure with PEG, and the crosslinking points are fixed. In addition, the figure-eight cross-linking of cyclodextrins on PEG chains makes the hydrogel have a sliding cross-linking point. Therefore, the constructed hydrogel possesses two types of crosslinked structures. However, if the general cross-linked hydrogels in the figure eight shape do not connect the cyclodextrins on the PEG, a relatively stable network structure cannot be constructed. In addition, the crosslinking of hydrogel terminated by photopolymerization can simplify the end-capping procedure. Herein, we wish to report a type of new slide-ring supramolecular hydrogel constructed from (2-hydroxypropyl)- α -CD (Hy- α -CD), which has good water solubility and biocompatibility^{33–36}, via a convenient photo-initiated polymerization with acrylamide-terminated polyethyleneglycol followed by the crosslink of Hy- α -CD sliding ring. In this work, Hy- α -CD/ACA-PEG₂₀₀₀₀-ACA hydrogel was prepared via a simple two-step reaction (Fig. 1). First, Hy- α -CD and ACA-PEG₂₀₀₀₀-ACA formed pseudopolyrotaxane in water through host-guest interactions, and this pseudopolyrotaxane subsequently converted

to the capped polyrotaxane by a simple photo-initiated polymerization in the presence of acrylamide and a little amount of I₂₉₅₉ in water. Then, polyrotaxane was further cross-linked in a sodium hydroxide solution of 1,4-butanediol diglycidyl ether to give a ultrastretchable supramolecular hydrogel, which was stretched to 2540% of its original length and has a fracture energy of 17.4 MJ/m³ as well as an elastic modulus of 35.67 KPa. Further experiment indicated this hydrogel can be used to prepare a wearable strain sensor with high performance after simply doped with 0.2 M CaCl₂ (to enhance the ions conductivity).

Results and discussion

Hydrogel synthesis. Hy- α -CD could be purchased commercially (Supplementary Fig. 1), and ACA-PEG₂₀₀₀₀-ACA was obtained through a three-step reaction (Supplementary Figs. 2, 3). A polypseudorotaxane could be constructed by mixing ACA-PEG₂₀₀₀₀-ACA and Hy- α -CD in water. In the two-dimensional (2D) ROESY spectrum (Supplementary Fig. 4), the signals assigned to 3-/5-H protons of Hy- α -CD at 4.00–3.75 ppm and PEG protons at 3.69 ppm showed the clear NOE correlations, indicating that the PEG chain is included in the cavities of Hy- α -CD. In addition, as shown in Supplementary Fig. 5, the gel was dialysated and then freeze-dried. The solid state NMR of freeze-dried samples was characterized. The NMR at the C5 of the cyclodextrin could be observed. This result demonstrates that the hydrogel still contained cyclodextrin units after dialysis, and the cyclodextrins were successfully capped by polyacrylamide. Subsequently, the capped polyrotaxane was obtained by a photo-initiated polymerization in-situ in the presence of a small amount of I₂₉₅₉ in water. In this process, a large amount of acrylamide monomer dissolved in water was copolymerized with a small amount of polypseudorotaxane modified by double bonds at both ends. Therefore, we could obtain polyrotaxane capped by polyacrylamide long chain. Furthermore, the dry weight of the end-capped polyrotaxane before and after soaked in excess water was compared, and the polymerization efficiency was calculated as > 90%. The high polymerization efficiency may come from the good solubility of acrylamide and pseudorotaxane in water, the system is completely transparent and there are no other substances competing to absorb UV light (see Supplementary Fig. 6). Such high polymerization efficiency also ensures the excellent mechanical properties of the slide-ring material obtained in the subsequent reaction to a certain extent. Immediately afterwards, the capped polyrotaxane was immersed in the sodium hydroxide solution of 1,4-butanediol glycidyl ether, where the concentration of 1,4-butanediol glycidyl ether is 20 wt%, and the concentration of sodium hydroxide is 1.5 M, to connect the discrete cyclodextrins by 1,4-butanediol glycidyl ether. In this way, the topologically figure-eight cross-linked slide-ring materials were prepared. By the way, the dry hydrogel could absorb about 60 times its own weight of water through the swelling experiment and remain stable in water for at least 15 days without being dissolved.

Characterization of Hy- α -CD/ACA-PEG₂₀₀₀₀-ACA hydrogel and Hy- α -CD/ACA-PEG₂₀₀₀₀-ACA/Ca hydrogel. The cross-sectional SEM images of the frozen-dried Hy- α -CD/ACA-PEG₂₀₀₀₀-ACA hydrogel and Hy- α -CD/ACA-PEG₂₀₀₀₀-ACA/Ca hydrogel showed the clear three-dimensional porous network structure (Fig. 2b, d), and the surface of Hy- α -CD/ACA-PEG₂₀₀₀₀-ACA hydrogel was relatively flat (Fig. 2a). As compared with Hy- α -CD/ACA-PEG₂₀₀₀₀-ACA hydrogel, the surface of the composite hydrogel doped with Ca²⁺ ions has a number of protrusions (Fig. 2c). When the hydrogel was deformed, the protrusions were stretched to protect the overall structure of the hydrogel, which enhanced the mechanical properties of the prepared hydrogels to

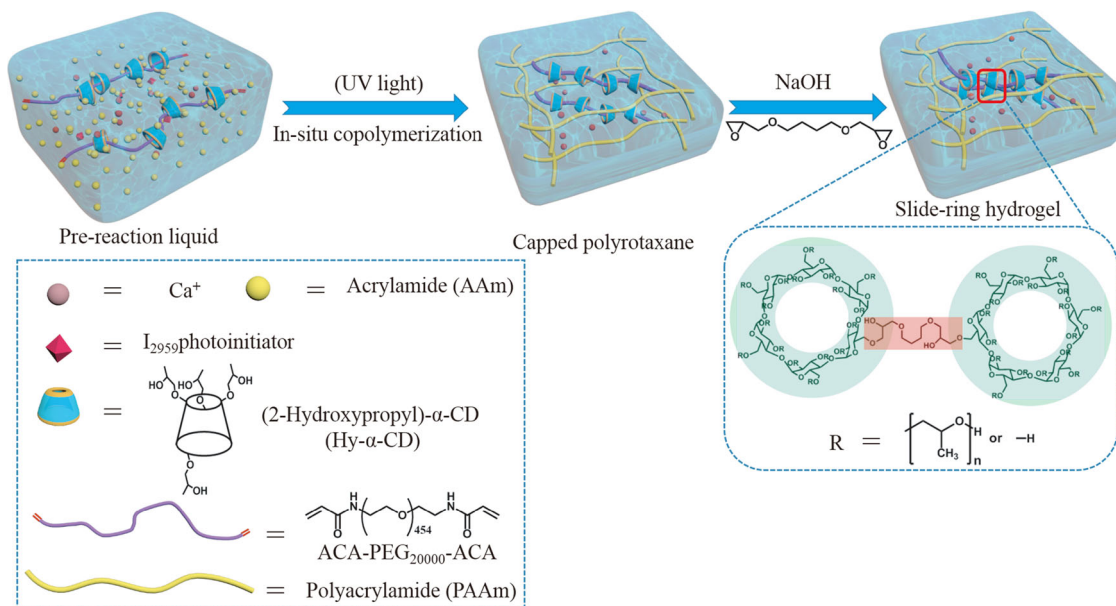


Fig. 1 Schematic illustration. Construction of Hy- α -CD/ACA-PEG₂₀₀₀₀-ACA/Ca hydrogel. (Formation of capped polyrotaxane by photopolymerization; formation of slide-ring hydrogel through further cross-linked cyclodextrins).

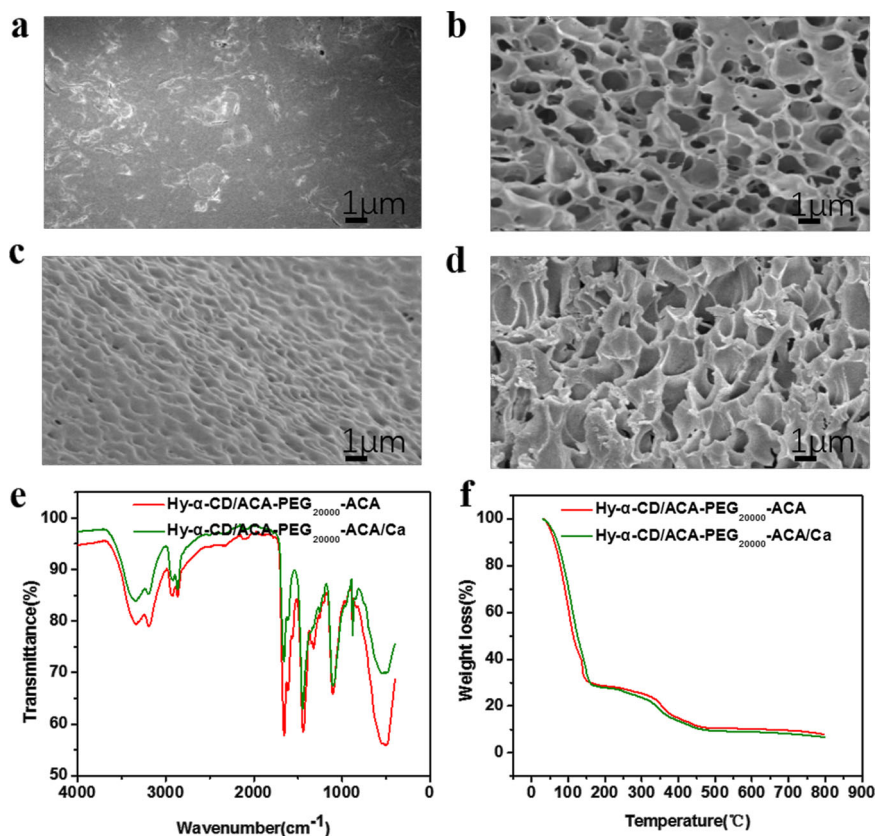


Fig. 2 SEM images, FT-IR spectra characterization and thermogravimetric analysis of hydrogels. **a** Surface SEM image of Hy- α -CD/ACA-PEG₂₀₀₀₀-ACA hydrogel. **b** Cross-sectional SEM image of Hy- α -CD/ACA-PEG₂₀₀₀₀-ACA hydrogel. **c** Surface SEM image of hydrogel doped with CaCl₂. **d** Cross-sectional SEM image of hydrogel doped with CaCl₂. **e** The FT-IR spectra of hydrogel (olive, hydrogel doped with CaCl₂; red, hydrogel doped without CaCl₂). **f** TG curves of hydrogel (olive, hydrogel doped with CaCl₂; red, hydrogel doped without CaCl₂).

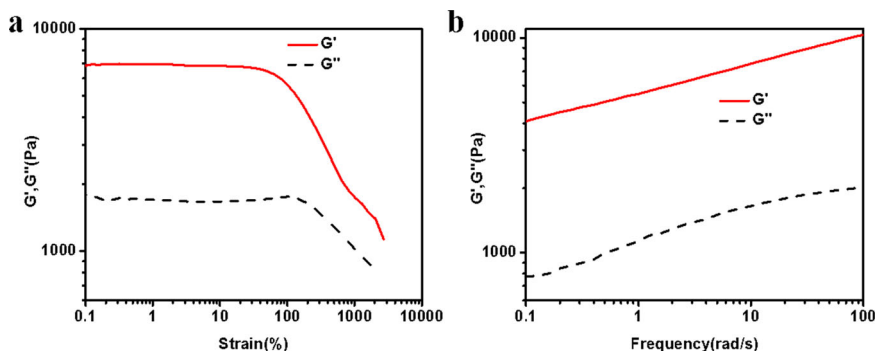


Fig. 3 Rheological characterization of the hydrogel. **a** G' (storage modulus) and G'' (loss modulus) as functions of strain. **b** G' and G'' as functions of frequency (ACA-PEG₂₀₀₀₀-ACA: Hy- α -CD = 1:5).

some extent (Supplementary Fig. 7). In the FT-IR spectra (Fig. 2e) of the hydrogel, the peaks at 3338.49 cm^{-1} , 3189.83 cm^{-1} , 1655.52 cm^{-1} , and 1613.35 cm^{-1} were assigned to the characteristic absorption of amides. The double peaks at 3338.49 cm^{-1} and 3189.83 cm^{-1} corresponded to the N-H stretching vibrations in acrylamide. The peak at 1655.52 cm^{-1} was assigned to the stretching vibration of C=O connected to -NH₂. The peak at 1613.35 cm^{-1} corresponded to the bending vibration of N-H. In the TG curves (Fig. 2f), the mass loss of Hy- α -CD/ACA-PEG₂₀₀₀₀-ACA hydrogel was 71.1% when the temperature rose from room temperature to $186\text{ }^{\circ}\text{C}$, which was mainly due to the evaporation of a large amount of water in the hydrogel. It is basically the same as the water content in the gel previously calculated. When the temperature rose from 200 to $300\text{ }^{\circ}\text{C}$, the second round of mass loss of the two gels occurred. The mass loss at this stage was caused by the condensation of adjacent amide groups on the long chain of the PAAm polymer. Many amino groups are removed to form imide groups⁴. Finally, when the temperature rose above $550\text{ }^{\circ}\text{C}$, the Hy- α -CD and PAAm begin to oxidize gradually and exotherm. Therefore, mass loss occurred again. The above data shows that the addition of metal ions will not destroy the thermodynamic stability of the hydrogels.

Rheological properties of the hydrogels. Rheological tests were also carried out to investigate the mechanical property of the hydrogels. It can be clearly seen from the Fig. 3a and Supplementary Fig. 8a, c that for three ratios of hydrogels (ACA-PEG₂₀₀₀₀-ACA: Hy- α -CD = 1:0; 1:5; 1:10), when the stress increased from 0.1% to 2000%, the storage modulus (G') was always greater than the loss modulus (G''). Especially for the case of ACA-PEG₂₀₀₀₀-ACA: Hy- α -CD = 1:5, G' was still greater than G'' even when the stress was 3000%. In the frequency sweep curve (Fig. 3b and Supplementary Fig. 8b, d), as the frequency increases from 0.1% to 100%, G' and G'' both gradually increased and remained parallel, and G' was always much larger than G'' . On the other hand, although the G' value of Hy- α -CD/PEG₂₀₀₀₀ hydrogel was larger than that of Hy- α -CD/ACA-PEG₂₀₀₀₀-ACA hydrogel when the strain increased from 0.1% to 300%, the Hy- α -CD/PEG₂₀₀₀₀ hydrogel would be destroyed when the strain is greater than 300% from Supplementary Fig. 4e, f. It may be because there are no double bonds at both ends of the polyethylene glycol in the Hy- α -CD/PEG₂₀₀₀₀ hydrogel, it is equivalent to no rotaxane crosslinker was added to the hydrogel. When polyethylene glycol without double bonds was used as a control molecule, the resultant polypseudorotaxane could not form a stable three-dimensional network structure with acrylamide. This makes acrylamide denser to a certain extent, so G' is relatively large at the beginning, but this structure is easily destroyed when the strain increases. This shows the importance of the rotaxane structure to improve the mechanical properties of hydrogels.

Mechanical properties of the hydrogels. In the tensile test of hydrogels (Fig. 4a, b, Supplementary Fig. 9), simply stretching by hand could easily stretch the Hy- α -CD/ACA-PEG₂₀₀₀₀-ACA hydrogel to 2540% of its original length, and it could instantly restore to 110% of its original length after the external force was released, indicating that the hydrogel had the high elasticity. In the tensile tests of a series of hydrogels with different ACA-PEG₂₀₀₀₀-ACA/Hy- α -CD ratios, the maximum stretching length of the hydrogel made from the free ACA-PEG₂₀₀₀₀-ACA could reach 2810%. In this case, the hydrogel has the highest ductility and toughness compared with the other two samples. On the one hand, the hydrogel has already formed a relatively complete network structure. On the other hand, because there is no crosslinked cyclodextrins, the crosslinking density is smaller, so that the gel is easier to stretch. Therefore, the ductility is better, the flexibility is stronger, but the tensile recovery ability is poor. However, the hydrogel made from the free ACA-PEG₂₀₀₀₀-ACA and Hy- α -CD showed the rapid recovery and strength. After the addition of cyclodextrins, the figure-eight cross-linked structure in the system makes the anti-fatigue performance more excellent. Although it decreases some ductility, it makes the tensile recovery ability of hydrogel better, so that the gel could recovery rapidly after stretching. As shown in Fig. 4c, the area of the hysteresis loops of the ACA-PEG₂₀₀₀₀-ACA/Hy- α -CD hydrogel was smaller than that of free ACA-PEG₂₀₀₀₀-ACA. When 5 equivalents of Hy- α -CD was added to ACA-PEG₂₀₀₀₀-ACA, the strength of the resultant hydrogel increased 0.5 MPa, while the strain at breaking only lost 9.6%. A possible reason may be that the addition of Hy- α -CD increased the cross-linking density of the hydrogel and thus enhanced the strength. In addition, these cyclodextrin molecules could slide freely on PEG chains without falling off, and the internal stress caused by stretching was thus greatly released. With further increasing the ratio of Hy- α -CD to 10 equivalent, although the gel strength slightly increased 0.3 MPa, the fracture strain loses 19.7% compared with the case of 1:5, which may be too many cyclodextrins on PEG chains greatly reduces the sliding range of a single cyclodextrin, resulting in a rapid increase in gel fragility. By calculating the fracture energy and elastic modulus, we can see that as the content of Hy- α -CD increases, the fracture energy of the hydrogel continuously decreases. When the ratio of ACA-PEG₂₀₀₀₀-ACA to Hy- α -CD is 1:5, the fracture energy only reduces 1.36 MJ/m^3 compared with the case of free ACA-PEG₂₀₀₀₀-ACA, but the elastic modulus increases 7.95 KPa (Fig. 4d, Supplementary Fig. 10). When the ratio of ACA-PEG₂₀₀₀₀-ACA to Hy- α -CD increases to 1:10, the fracture energy decreases 7.65 MJ/m^3 , but the elastic modulus increases $< 4\text{ KPa}$, compared with that of ACA-PEG₂₀₀₀₀-ACA: Hy- α -CD = 1:5. That is, when the ratio of cyclodextrin is five equivalents, the hydrogel has not only a high breaking energy as 17.4 MJ/m^3 but also an ultra-high elastic modulus as 35.67 KPa . These values are

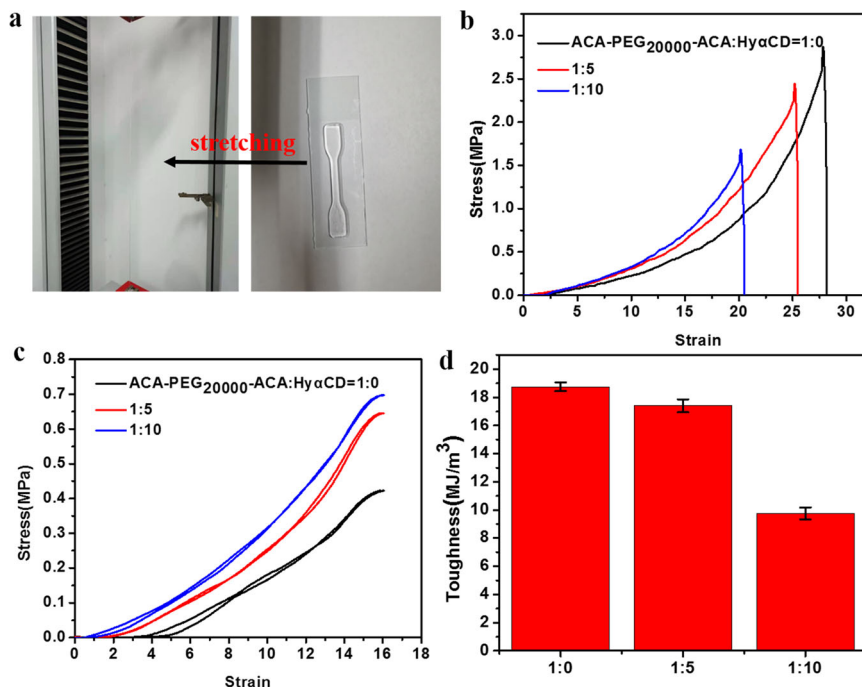


Fig. 4 Tensile properties of hydrogels. **a** Visual photos used to show the excellent ductility (ACA-PEG₂₀₀₀₀-ACA: Hy- α -CD = 1:5) and Optical photographs of the stretching of the hydrogel. **b** Tensile stress–strain curves of hydrogels with different polypseudorotaxane components. (black, ACA-PEG₂₀₀₀₀-ACA: Hy- α -CD = 1:0; red, ACA-PEG₂₀₀₀₀-ACA: Hy- α -CD = 1:5; blue, ACA-PEG₂₀₀₀₀-ACA: Hy- α -CD = 1:10). **c** Tensile loading–unloading curves of hydrogels with different polypseudorotaxane components at strain of 1600% (samples represented by different colors are the same as in Fig. 3c). **d** Fracture energy of Hy- α -CD/ACA-PEG₂₀₀₀₀-ACA hydrogel with the ACA-PEG₂₀₀₀₀-ACA: Hy- α -CD ratio of 1:0, 1:5 and 1:10.

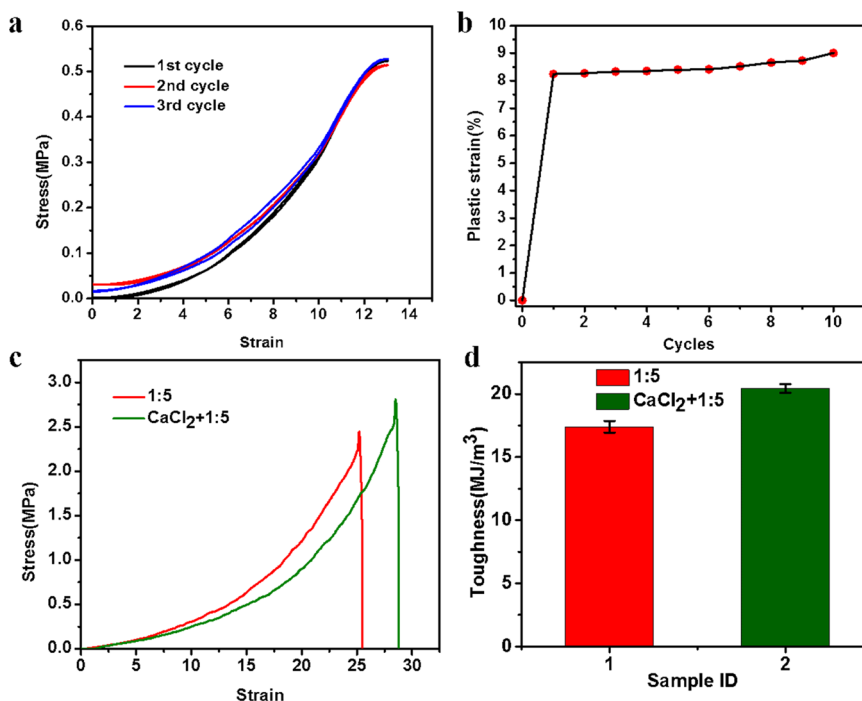


Fig. 5 Tensile recovery properties of hydrogels and effects of ions on mechanical properties of hydrogels. **a** Cyclic loading–unloading tensile curves of the Hy- α -CD/ACA-PEG₂₀₀₀₀-ACA hydrogel (ACA-PEG₂₀₀₀₀-ACA: Hy- α -CD = 1:5) at 1300% strain for three cycles (no waiting time between cycles). **b** Plastic strain as a function of cycle times at strain of 1100% (no waiting time between cycles, ACA-PEG₂₀₀₀₀-ACA: Hy- α -CD = 1:5). **c** Tensile stress–strain curves of hydrogel doped with CaCl₂ compared with the hydrogel without CaCl₂ (ACA-PEG₂₀₀₀₀-ACA: Hy- α -CD = 1:5). **d** Fracture energy of hydrogel doped with CaCl₂ compared with the hydrogel without CaCl₂ (ACA-PEG₂₀₀₀₀-ACA: Hy- α -CD = 1:5). (Error bars indicate the average value and certain error obtained from three experiments for every sample).

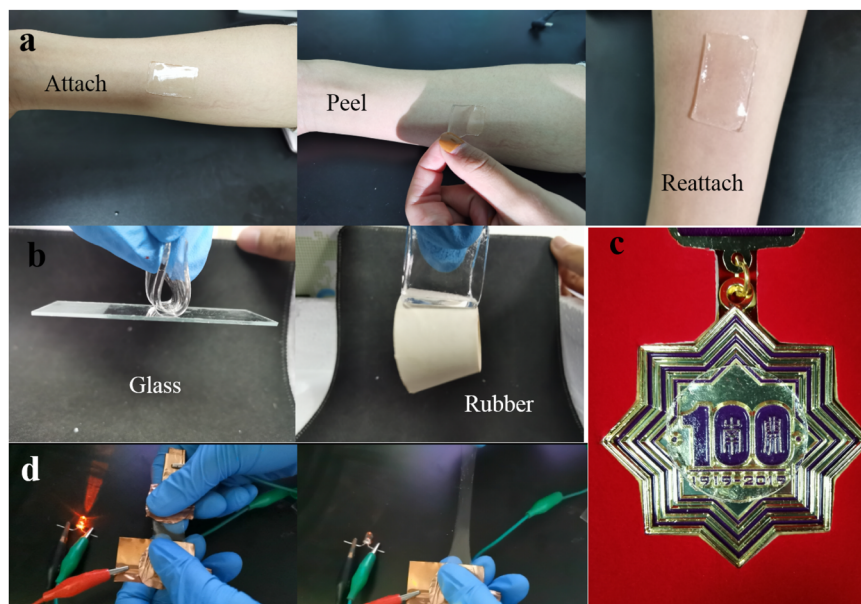


Fig. 6 Adhesion and conductivity test of hydrogel. **a** Hydrogel could adhere to the skin. (Hy- α -CD-ACA-PEG₂₀₀₀₀-ACA/Ca hydrogel; ACA-PEG₂₀₀₀₀-ACA: Hy- α -CD = 1:5). **b** The hydrogel exhibited universal adhesiveness on material surfaces of glass and rubber. **c** Optical photo of a transparent hydrogel covering the Nankai University 100th Anniversary emblem. **d** Hydrogel could conduct electricity to brighten the bulb, and the bulb would become darker when the hydrogel was stretched.

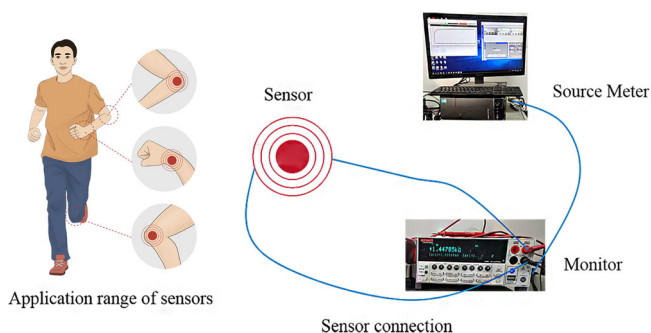


Fig. 7 The sensing application of strain sensors and the composition and signal conversion process of strain sensors. After receiving the human motion signal, the sensor is monitored by the detector (monitor; source meter), and then processed by the processor (computer) and converted into a digital signal.

higher than those of most of reported hydrogels with such high water content. Owing to the high breaking energy, the hydrogel is hard to be broken when it is applied to the sensor, and the ultra-high elastic modulus ensures that the sensor can recover in time after being stretched.

In order to investigate the anti-fatigue performance of the hydrogel, the loading-unloading tensile test of the hydrogel under the condition of 1300% maximum strain was performed. As shown in Fig. 5a, during the first cycle, the integral area of the hysteresis loop reached 0.026 MJ/m^3 . In the subsequent cycles, the hydrogel could almost be restored to its original state. The corresponding area of the hysteresis loops was $<0.15 \text{ MJ/m}^3$. The reason may be that a small amount of polypseudorotaxane cross-linking agent in the hydrogel is not fully reacted and has not been capped, and these unstable structures will be irreversibly destroyed during the first few stretching processes. To visually illustrate the superior fatigue resistance of the hydrogel, we tested the plastic strain value of the hydrogel after 1100% strain reciprocating many times. As shown in Fig. 5b, the hydrogel

experienced 8.3% plastic strain after the initial cycle, and this value quickly stabilized afterwards, and finally did not exceed 10% after 10 cycles. In order to clarify the influence of CaCl_2 on the mechanical properties of the hydrogel, we compared its mechanical properties with the hydrogel without CaCl_2 . The result show that its tensile strength, maximum elongation, and fracture energy increased 14.6%, 13.4%, and 17.5%, respectively, compared with the corresponding Hy- α -CD/ACA-PEG₂₀₀₀₀-ACA hydrogel (Fig. 5c, d, Supplementary Figs. 11, 12). This may be mainly because the addition CaCl_2 introduced ionic bonds on the basis of the original covalent bonds, so that the excellent recovery performance of the hydrogel was completely preserved. Due to the high elasticity and excellent recovery performance of the hydrogel, the prepared strain sensor also has good stretching and deformation properties. In addition, when CaCl_2 is added, the maximum stretch length of the hydrogel can reach 2880%. When the hydrogel is applied to the sensor, its good ductility allows the sensor to monitor the movement of the human body over a larger range. At the same time, the hydrogel sensor is not easy to be broken and has better fatigue resistance, ensuring that the sensor can be used repeatedly.

Testing of strain sensors. It is well-known that the preparation of a hydrogel into a strain sensor needs to meet conditions such as adhesion and high transparency. The ACA-PEG₂₀₀₀₀-ACA/Hy- α -CD hydrogel displayed the satisfactory adhesion on some material surfaces. As shown in Fig. 6b, the hydrogel could easily adhere to glass and rubber. Importantly, the hydrogels not only exhibited the good adhesive behavior on human skin and could be adhered again after peeling off but also could be removed without any residue, irritation, or allergy reaction (Fig. 6a)³⁷. Although we have not been able to directly measure the adhesion strength of the gel, we tried the adhesion properties of the gel to different substances under a certain contact area, showing a certain degree of adhesion. For example, when the contact area between the gel and the substrates is 130 mm^2 , 5 grams of glass or 9.5 grams of rubber can adhere to the gel, and can be maintained for more than two minutes without falling off. In Fig. 6c, we can

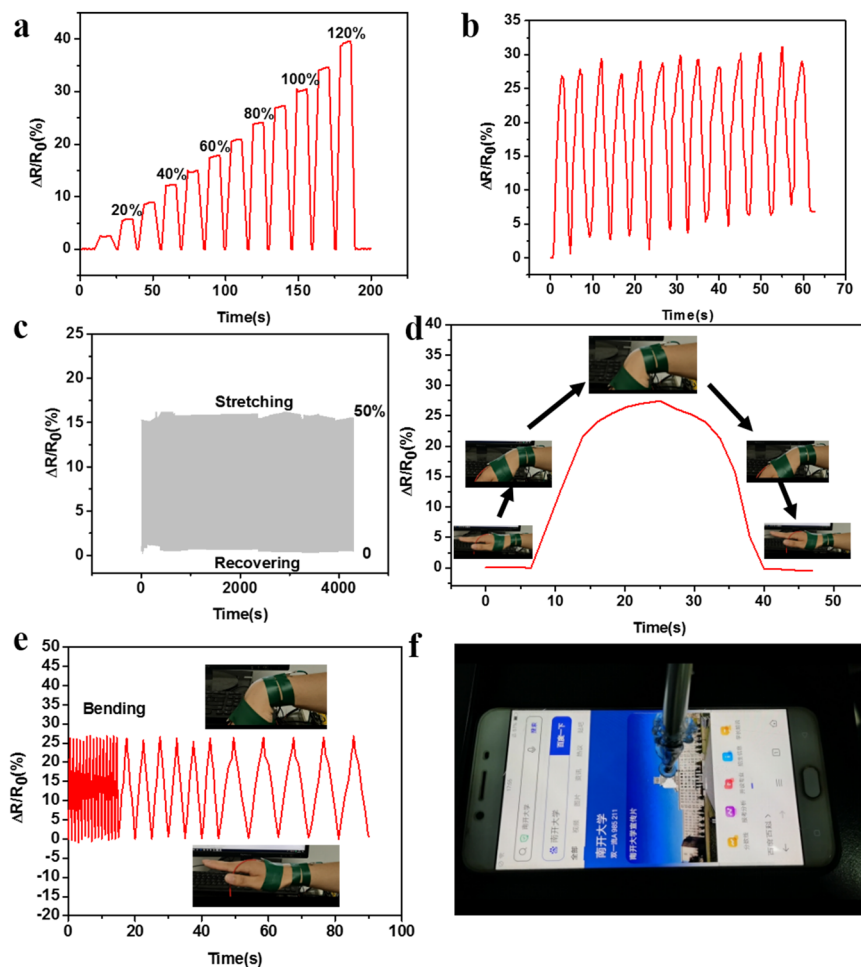


Fig. 8 The sensing performance of hydrogels and the control of electronic screen. **a** $\Delta R/R_0$ curves of the hydrogel under different tensile strains (ACA-PEG₂₀₀₀₀-ACA: Hy- α -CD = 1:5). **b** $\Delta R/R_0$ curves of the hydrogel during the stretching-recovery cycle when the tensile strain is 90%. **c** The $\Delta R/R_0$ curve of the hydrogel under 300 cycles of load-unload. **d** Real-time signal of the wrist movement. **e** At different bending speeds. **f** Image of the phone controlled by the conductive hydrogels.

clearly see the fonts and colors covered under the hydrogel, demonstrating that the hydrogel has the good optical transparency. Due to the presence of Ca^{2+} and Cl^- ions, the hydrogel shows the good ionic conductivity. In a conductivity experiment, the hydrogel can conduct electricity to brighten the bulb, and the bulb will become darker when the hydrogel is stretched (Fig. 6d, Supplementary Movie 1).

Owing to the conductivity, robust adhesiveness and high stretchability, the hydrogel is regarded as a potential material for flexible wearable sensors and can be designed as a wearable strain sensor for monitoring human motions (Fig. 7). In order to evaluate the sensitivity of the hydrogel as a strain sensor, the relative resistance change of the hydrogel under different strains was investigated. As the strain increased from 0% to 120%, the electrical resistance of the hydrogel exhibited an obvious step-like increasing trend (Fig. 8a). The hydrogel was capable of restoring to its original shape after being released with the resistance turning into its initial value. Moreover, the electrical resistance of the hydrogel maintained a constant value during the stretching-holding and bending-holding process. These results indicate the high strain sensitivity and the good electrical stability of the hydrogel strain sensor. It can be seen from Fig. 8b that the overall fluctuation range of $\Delta R/R_0$ (%) in the 13 exercise cycles is very small, indicating that the Hy- α -CD/ACA-PEG₂₀₀₀₀-ACA/Ca hydrogel can better reflect the action state when the amplitude

of the action is large. In Fig. 8c, after 300 cycles at 0–50% tensile strain, the strain sensor also showed the good stability, indicating that the hydrogel still maintained a complete structure and the electrical sensitivity. The introduction of the chemically cross-linked network preserves the overall morphology of the hydrogel. The ion-crosslinked network can effectively disperse the energy generated by stretching and make the resistance of the hydrogel sensor change regularly when the strain occurs. A robust adhesion between hydrogel sensors and the human skin is vital to effectively detect and transport electrical signals under repeated deformation. The excellent adhesiveness of the hydrogels allowed the good attachment to the bended skin surface to detect the dynamic process of human motions. Figure 8d and Supplementary Movie 2 show the change of $\Delta R/R_0$ (%) of the hydrogel sensor during the wrist movement. By attaching the hydrogel strain sensor directly to the wrist, it was not difficult to find that the relative resistance changes of the hydrogel exhibited different levels under different bending angles, and the $\Delta R/R_0$ (%) of the hydrogel increased with the increase of the bending angle. At the same time, when returning to the original position, the change in resistance would be completely reduced to its initial value. Furthermore, the hydrogel sensor could also quickly respond to different strain speeds. Figure 8e shows the relative resistance variation curve of the hydrogel at different bending speeds when the wrist was bent. As the bending frequency decreased, the

curves of relative resistance change becomes from dense to sparse. These results verify the high strain sensitivity and the ultra-fast response capability of the hydrogel sensors (see Supplementary Fig. 13).

In addition, it is not difficult to find that the application of flexible electronic materials to some screen control is a direction of future development. Therefore, whether the hydrogel strain sensor can be applied to the touch control of electronic screen was explored. After the hydrogel was wrapped on the tip of the electronic pen (Supplementary Fig. 14), it was found that the phone screen could still be manipulated by touching the screen without any obstacles (Fig. 8f and Supplementary Movie 3). This property demonstrated that the hydrogel material was also available for the human-computer interactions. Furthermore, because the hydrogel is smooth and soft, it can also prevent the screen from scratching. These researches provided new ideas for the preparation and application of slide-ring materials.

Conclusion

In summary, we successfully constructed a slide-ring hydrogel by Hy- α -CD and ACA-PEG₂₀₀₀₀-ACA, which shows high stretchability (2540%), high elastic modulus (35.67 KPa), high toughness (17.4 MJ/m³) and good recovery property (Supplementary Fig. 15). After CaCl₂ was added, the slide-ring hydrogel not only retains the good mechanical properties but also showed the enhanced ionic conductivity, and thus can be successfully applied to the flexible wearable strain sensors. Further experiments show the hydrogel material was also available for operating device of the human-computer touching.

Methods

Reagents and materials. Polyethylene glycol (PEG₂₀₀₀₀), P-toluenesulfonyl chloride, magnesium sulphate and 2-hydroxy-4'-(2-hydroxyethoxy)-2-methyl propiophenone (I₂₉₅₉) were purchased from Tianjin Heowns Biochemical Technology Co., Ltd. Acrylamide (AAm) and Triethylamine (TEA) were purchased from Kmart (Tianjin) Chemical Technology Co., Ltd. Calcium chloride (CaCl₂), dehydrate, were purchased from Shanghai Aladdin Biochemical Technology Co., Ltd. (2-hydroxypropyl)- α -CD (Hy- α -CD) were purchased from Beijing Huawei Ruike Chemical Co., Ltd. and other solvents were purchased from Beijing Bailingwei Technology Co., Ltd. without further purification. ACA-PEG₂₀₀₀₀-ACA was prepared according to reported literature synthesis (Scheme S1). All 1H NMR spectra and 2D ROESY spectra were recorded on a Bruker AV400 spectrometer. The microscopic morphology of the hydrogel was obtained on a JSM-7500F scanning electron microscope (SEM). The infrared spectra of the dry gel was recorded on TENSOR II Fourier transform infrared spectrometer. Thermogravimetric (TG) analysis was finished in an argon at mosphere using a Netzsch STA 409 PC Luxx simultaneous thermal analyzer. Disc-shaped samples with thicknesses of 2 mm and diameters of 20 mm were used to perform the rheological tests on an AR 2000ex (TA Instrument) system at 20 °C.

Preparation of Hy- α -CD/ACA-PEG₂₀₀₀₀-ACA Poly-pseudorotaxane. A total of 200 mg of ACA-PEG₂₀₀₀₀-ACA was dissolved in 10 mL of deionized water, and then a corresponding ratio of Hy- α -CD was added. After an ultrasonic treatment for 30 min, the mixture was allowed to stand at room temperature for 6 days to obtain a nearly transparent suspension.

Preparation of capped Hy- α -CD/ACA-PEG₂₀₀₀₀-ACA polyrotaxane. One mL of well-shaken Hy- α -CD/ACA-PEG₂₀₀₀₀-ACA polypseudorotaxane suspension was added to a sample tube with 3 mL of 300 mg/mL acrylamide aqueous solution and then 5 mg of I₂₉₅₉ was added to the system. After shaking up the tube until the mixture became clear, the mixture was transfer to a teflon mold, covered with a glass coverslip, and irradiated under UV light (365 nm) for 15 min to get the capped Hy- α -CD/ACA-PEG₂₀₀₀₀-ACA polyrotaxane. For the preparation capped Hy- α -CD/ACA-PEG₂₀₀₀₀-ACA polyrotaxane doped with CaCl₂, 0.2 M CaCl₂ was added in the pre-reaction mixture, and the other operations were unchanged.

Preparation of Hy- α -CD/ACA-PEG₂₀₀₀₀-ACA hydrogel. The capped polyrotaxane was immersed in a sodium hydroxide solution (1.5 M) containing 20 wt% 1,4-butanediol glycidyl ether and left standing at room temperature for 20 h to form a slide-ring hydrogel.

Swelling experiments. The swelling experiments were performed by immersing the dry gel in a large excess of water in beaker at room temperature until it stop swelling.

Tensile strength measurement. Samples for tensile strength measurements were rectangular shapes with a size of 40 × 4 × 2 mm, and the tensile speed was 100 mm/min. Tensile strength was tested on a universal test machine AG-10TA at room temperature (25 °C).

Preparation and test of strain sensors. The sensitivity of a strain sensor can be reflected by changes in resistance. The Keithley 2400 SourceMeter SMU (A Tektronix Company) produced by Panyuliang Instrumentation (Shanghai) Co., Ltd. was used to characterize the resistance change of the sensor. For the strain sensor to sense strain, the hydrogels doped with CaCl₂ were made into a rectangular sample with a length of 40 mm, a width of 20 mm, and a thickness of 2 mm. When assembling the sensor and the test instrument, we connected copper wires to the wires at both ends of the sample.

Calculation of fracture energy. According to a previous method of calculating fracture energy³⁸, tensile toughness determined by integrating the area under stress-strain curves up to the specimen braking point.

Data availability

The data supporting the results of this study can be obtained from the corresponding author upon reasonable request.

Received: 3 October 2021; Accepted: 3 January 2022;

Published online: 20 January 2022

References

- Ohm, Y. et al. An electrically conductive silver-polyacrylamide-alginate hydrogel composite for soft electronics. *Nat. Electronic.* **4**, 185–192 (2021).
- Wang, Z. et al. A rapidly self-healing host-guest supramolecular hydrogel with high mechanical strength and excellent biocompatibility. *Angew. Chem. Int. Ed.* **57**, 9008–9012 (2018).
- Zhang, Y.-M., Liu, Y.-H. & Liu, Y. Cyclodextrin-based multistimuli-responsive supramolecular assemblies and their biological functions. *Adv. Mater.* **32**, 1806158 (2020).
- Bai, J. et al. Facile preparation and high performance of wearable strain sensors based on ionically cross-linked composite hydrogels. *Sci. China Mater.* **64**, 942–952 (2021).
- Zhang, Q., Liu, X., Duan, L. & Gao, G. Ultra-stretchable wearable strain sensors based on skin-inspired adhesive, tough and conductive hydrogels. *Chem. Eng. J.* **365**, 10–19 (2019).
- Rong, Q. et al. Anti-freezing, conductive self-healing organohydrogels with stable strain-sensitivity at subzero temperatures. *Angew. Chem. Int. Ed.* **56**, 14159–14163 (2017).
- Yan, X. et al. Quadruple H-bonding cross-linked supramolecular polymeric materials as substrates for stretchable, antitearing, and self-healable thin film electrodes. *J. Am. Chem. Soc.* **140**, 5280–5289 (2018).
- Zhang, K. et al. Polymerizable deep eutectic solvent-based mechanically strong and ultra-stretchable conductive elastomers for detecting human motions. *J. Mater. Chem. A.* **9**, 4890 (2021).
- Patel, D. K. et al. Highly stretchable and UV curable elastomers for digital light processing based 3D printing. *Adv. Mater.* **29**, 1606000 (2017).
- Wirthl, D. et al. Instant tough bonding of hydrogels for soft machines and electronics. *Sci. Adv.* **3**, e1700053 (2017).
- Qin, H., Zhang, T., Li, N., Cong, H.-P. & Yu, S.-H. Anisotropic and self-healing hydrogels with multi-responsive actuating capability. *Nat. Commun.* **10**, 2202 (2019).
- Li, W., Gao, F., Wang, X., Zhang, N. & Ma, M. Strong and robust polyaniline-based supramolecular hydrogels for flexible supercapacitors. *Angew. Chem. Int. Ed.* **55**, 9196–9201 (2016).
- Zhang, W., Zhang, Y.-M. & Liu, Y. Cyclodextrin-cross-linked hydrogels for adsorption and photodegradation of cationic dyes in aqueous solution. *Chem. Asian J.* **16**, 2321–2327 (2021).
- Deng, Z., Guo, Y., Zhao, X., Ma, P. X. & Guo, B. Multifunctional stimuli-responsive hydrogels with self-healing, high conductivity, and rapid recovery through host-guest interactions. *Chem. Mater.* **30**, 1729–1742 (2018).
- Liang, Y., Xue, J., Du, B. & Nie, J. Ultrastiff, tough, and healable ionic-hydrogen bond cross-linked hydrogels and their uses as building blocks to construct complex hydrogel structures. *ACS Appl. Mater. Interfaces.* **11**, 5441–5454 (2019).

16. Sun, G., Li, Z., Liang, R., Weng, L.-T. & Zhang, L. Super stretchable hydrogel achieved by non-aggregated spherulites with diameters <5 nm. *Nat. Commun.* **7**, 12095 (2016).
17. Feng, J.-F. et al. Leeches-inspired hydrogel–elastomer integration materials. *ACS Appl. Mater. Interfaces.* **10**, 40238–40245 (2018).
18. Gao, G., Du, G., Sun, Y. & Fu, J. Self-healable, tough, and ultrastretchable nanocomposite hydrogels based on reversible polyacrylamide/montmorillonite adsorption. *ACS Appl. Mater. Interfaces.* **7**, 5029–5037 (2015).
19. Lin, S. T. et al. Anti-fatigue–fracture hydrogels. *Sci. Adv.* **5**, eaau8528 (2019).
20. Wang, Y. J. et al. Ultrastiff and tough supramolecular hydrogels with a dense and robust hydrogen bond network. *Chem. Mater.* **31**, 1430–1440 (2019).
21. Kureha, T. et al. Decoupled thermo- and pH-responsive hydrogel microspheres cross-linked by rotaxane networks. *Angew. Chem. Int. Ed.* **56**, 15393–15396 (2017).
22. Tan, Y. J. et al. A transparent, self-healing and high- κ dielectric for low-field-emission stretchable optoelectronics. *Nat. Mater.* **19**, 182–188 (2020).
23. Liu, Y. et al. Highly flexible and resilient elastin hybrid cryogels with shape memory, injectability, conductivity, and magnetic responsive properties. *Adv. Mater.* **28**, 7758–7767 (2016).
24. Yang, Y., Wang, X., Yang, F., Shen, H. & Wu, D. A universal soaking strategy to convert composite hydrogels into extremely tough and rapidly recoverable double-network hydrogels. *Adv. Mater.* **28**, 7178–7184 (2016).
25. Hua, M. et al. Strong tough hydrogels via the synergy of freeze-casting and salting out. *Nature.* **590**, 594–599 (2021).
26. Katsuno, C. et al. Pressure-responsive polymer membranes of slide-ring gels with movable cross-links. *Adv. Mater.* **25**, 4636–4640 (2013).
27. Choi, S., Kwon, T.-W., Coskun, A. & Choi, J. W. Highly elastic binders integrating polyrotaxanes for silicon microparticle anodes in lithium ion batteries. *Science.* **357**, 279–283 (2017).
28. Lin, Q., Hou, X. & Ke, C. Ring shuttling controls macroscopic motion in a three-dimensional printed polyrotaxane monolith. *Angew. Chem. Int. Ed.* **56**, 4452–4457 (2017).
29. Yasuda, Y. et al. Molecular dynamics of polyrotaxane in solution investigated by quasi-elastic neutron scattering and molecular dynamics simulation: sliding motion of rings on polymer. *J. Am. Chem. Soc.* **141**, 9655–9663 (2019).
30. Gotoh, H. et al. Optically transparent, high-toughness elastomer using a polyrotaxane cross-linker as a molecular pulley. *Sci. Adv.* **4**, eaat7629 (2018).
31. Li, Z., Zhang, Y.-M., Wang, H.-Y., Li, H. & Liu, Y. Mechanical behaviors of highly swollen supramolecular hydrogels mediated by pseudorotaxanes. *Macromolecules* **50**, 1141–1146 (2017).
32. Imran, A. B. et al. Extremely stretchable thermosensitive hydrogels by introducing slide-ring polyrotaxane cross-linkers and ionic groups into the polymer network. *Nat. Commun.* **5**, 5124 (2014).
33. Feng, L., Jia, S.-S., Chen, Y. & Liu, Y. Highly elastic slide-ring hydrogel with good recovery as stretchable supercapacitor. *Chem. Eur. J.* **26**, 14080–14084 (2020).
34. Li, Z., Zheng, Z., Su, S., Yu, L. & Wang, X. Preparation of a high-strength hydrogel with slidable and tunable potential functionalization sites. *Macromolecules* **49**, 373–386 (2016).
35. Jiang, L. et al. Highly stretchable and instantly recoverable slide-ring gels consisting of enzymatically synthesized polyrotaxane with low host coverage. *Chem. Mater.* **30**, 5013–5019 (2018).
36. Liu, C. et al. Tough hydrogels with rapid self-reinforcement. *Science* **372**, 1078–1081 (2021).
37. Mo, J. et al. Design of ultra-stretchable, highly adhesive and self-healable hydrogels via tannic acid-enabled dynamic interactions. *Mater. Horiz.* **8**, 3409–3416 (2021).
38. Peng, H. et al. Ultra-stretchable hydrogels with reactive liquid metals as asymmetric force-sensors. *Mater. Horiz.* **6**, 618–625 (2019).

Acknowledgements

This work was financially supported by the National Natural Science Foundation of China (grant nos. 22131008 and 21971127).

Author contributions

Y.L., Y.C., and S.W. conceived and designed the experiments. S.W. synthesized and performed the chemical characterization. Y.S., Y.Q., H.Z., and X.Y. conducted the strain sensors experiments. S.W. wrote the main manuscript. Y.L. supervised the work and edited the manuscript. All authors analyzed and discussed the results and reviewed the manuscript.

Competing interests

The authors declare no competing interests.

Additional information

Supplementary information The online version contains supplementary material available at <https://doi.org/10.1038/s43246-022-00225-7>.

Correspondence and requests for materials should be addressed to Yu Liu.

Peer review information *Communications Materials* thanks Xuzhou Yan, Jiheong Kang and the other, anonymous, reviewer for their contribution to the peer review of this work. Primary Handling Editors: Jie Xu and John Plummer. Peer reviewer reports are available.

Reprints and permission information is available at <http://www.nature.com/reprints>

Publisher's note Springer Nature remains neutral with regard to jurisdictional claims in published maps and institutional affiliations.



Open Access This article is licensed under a Creative Commons Attribution 4.0 International License, which permits use, sharing, adaptation, distribution and reproduction in any medium or format, as long as you give appropriate credit to the original author(s) and the source, provide a link to the Creative Commons license, and indicate if changes were made. The images or other third party material in this article are included in the article's Creative Commons license, unless indicated otherwise in a credit line to the material. If material is not included in the article's Creative Commons license and your intended use is not permitted by statutory regulation or exceeds the permitted use, you will need to obtain permission directly from the copyright holder. To view a copy of this license, visit <http://creativecommons.org/licenses/by/4.0/>.

© The Author(s) 2022